N88-13626

A System Identification Technique Based on the Random Decrement Signatures Part II: Experimental Results

Nabih E. Bedewi
Jackson C. S. Yang

Identification of the system parameters of a randomly excited structure may be treated using a variety of statistical techniques. Of all these techniques, the Random Decrement is unique in that it provides the homogeneous component of the system response. Using this quality, a system identification technique was developed based on a least-squares fit of the signatures to estimate the mass, damping, and stiffness matrices of a linear randomly excited system. In part I of this paper the mathematics of the technique was presented in addition to the results of computer simulations conducted to demonstrate the prediction of the response of the system and the random forcing function initilly introduced to excite the system. This part of the paper presents the results of an experiment conducted on an offshore platform scale model to verify the validity of the technique and to demonstrate its application in damage detection.

INTRODUCTION

A system identification technique was developed in part I of this paper for extracting meaningful information from randomly excited structures. This technique is based on the Random Decrement and cross-Random Decrement signatures of the structure [2,3,4,5]. Computer simulations performed using a linear system demonstrated the effectiveness of this technique in obtaining an accurate model of the system and in predicting the random forcing function introduced for excitation. The system identification technique is briefly desrcibed as follows:

Given a randomly excited linear multidegree-of-freedom system, response data is obtained at several locations. A model for the system is assumed in the form

$$[M]\ddot{X} + [C]\dot{X} + [K]X = F \qquad (1)$$

where [M] and [K] are real symmetric matrices representing the mass and stiffness of the structure, [C] is a nonproportional , real, symmetric damping matrix, **F** is the forcing vector, and **X** and its time derivatives represent the response of the system. Random Decrement and cross-Random Decrement signtuares are then obtained from the response data thus forming the homogeneous components of the response. Substituting the signatures in Equation (1) and noting that vector **F** is zero, a least squares fit is then performed with the assumption that one of the elements in the system matrices is known. A detailed description of the constraints on the matrices and the least squares method is given in part I of this paper.

SCALE MODEL EXPERIMENT

A 1 : 13.8 scale model of an offshore platform structure was set up on outdoor earth ground. The base of the structure was welded to a steel (box type) frame, then both were lowered into a 6'x6'x3' pit hole. The pit was then filled with wet concrete up to the the base of the structure and left to cure.

The model structure consists of four legs made of 2" diameter, 0.25" wall, steel pipes. Figure 1 shows the configuration of the structure with its dimensions and labeled points. A pendulum was set up to provide random impact excitation at point 13. The responses at points 1 to 13 were monitored using accelerometers screwed into threaded aluminum blocks attached directly to the structure.

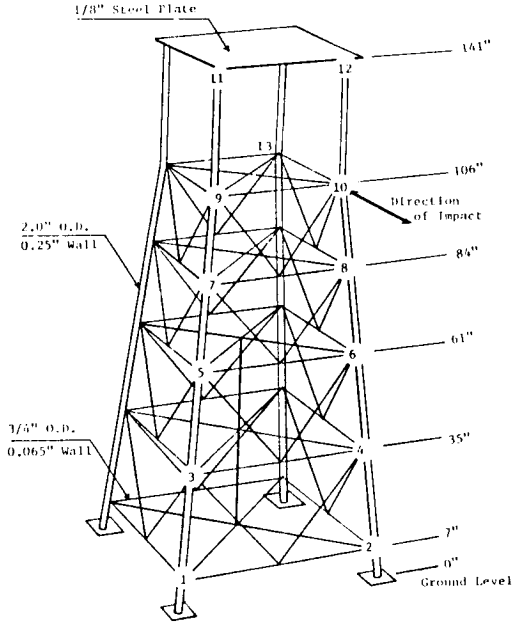

Figure 1 - Configuration of offshore platform scale model

VERIFICATION OF THE SYSTEM IDENTIFICATION TECHNIQUE

The first experiment was conducted to verify the reliability of the system identification technique in obtaining a model from Randomdec signatures. To accomplish this task, the response of the structure, as well as the input to the structure, had to be measured.

Four accelerometers were mounted at locations 4, 6, 8, and 13, and a load cell was firmly attached to the tip of the pendulum hammer. The structure was randomly impacted for 20 seconds while the output of the five transducers was recorded on analog tape simultaneously. The five channels were then digitized at a sampling rate of 1000 Hz after passing through a low pass filter set at 125 Hz. The cutoff frequency of the filter was selected based on a maximum system frequency of interest of 85 Hz.

The time record at location 13 was used for triggering the signatures. Figure 2 shows the Randomdec signature for location 13. The system identification technique was then employed in conjunction with the signatures to calculate the 30 unknown parameters in the [M], [C], [K] matrices. Four sets of matrices were initially calculated, each set corresponding to one fixed element in the stiffness matrix. The four sets of matrices were then averaged to obtain the best estimate for the model.

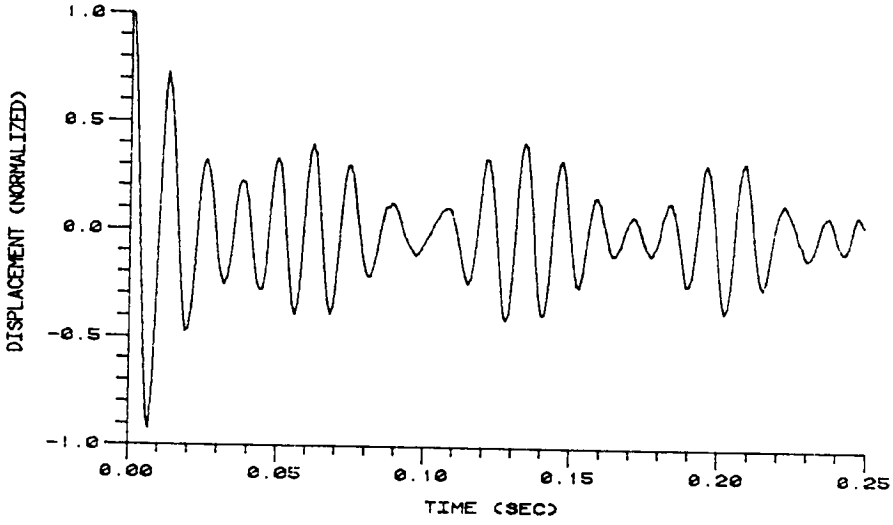

Figure 2 - Randomdec signature of time response at location 13

To confirm the accuracy of the established model, the three system matrices were substituted into the set of differential equations describing the system, Equation (1), and the second derivative of the load applied during the experiment introduced as input (the derivative is taken since the signatures were obtained from acceleration records). The initial conditions were extracted from the measured response of the system, and Equation (1) solved numerically. A step size of 0.001 sec. was used corresponding to the time step of the sampled data.

Since the estimated system parameters were not originally scaled to match the actual system in magnitude, the response had to be scaled to fascilitate the comparison. This was performed by multiplying the estimated reponses at the four points by the average of the ratios of the standard deviations of the measured responses to the standard deviations of the estimated responses. Furthermore, all the responses were multiplied by -1 since they appeared to be mirror images of the actual reponses about the time axis. This change in sign is a legitimate step since the same effect could have been achieved by scaling the system matrices by -1.

The results of the comparison at point 4 are shown in Figure 3. The plots indicate that the predicted system response is in good agreement with the actual response.

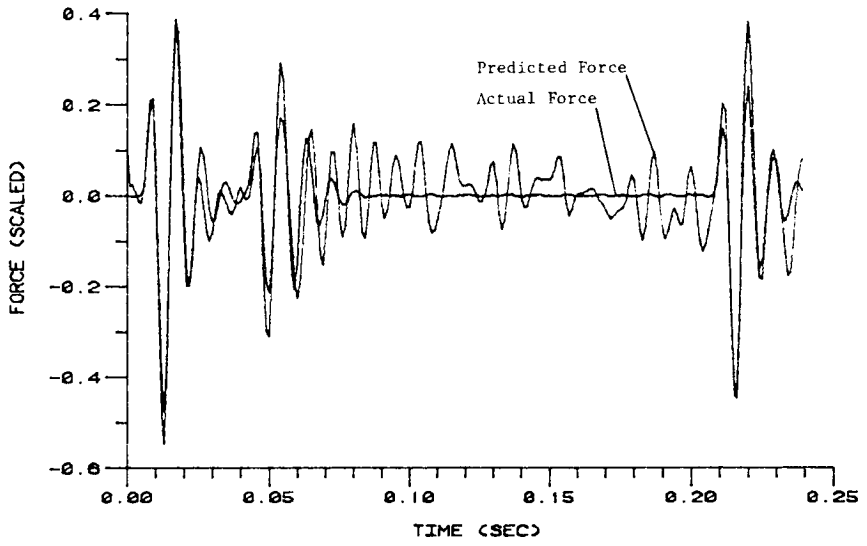

Figure 3 - Comparison of measured vs. predicted responses at point 4

Another approach to verify the accuracy of the model is to compare the measured force with the predicted force. Therefore, the measured system response was substituted in Equation (1) with the three estimated matrices and the force vector calculated. Again, the output was scaled for comparison. Figure 4 shows the predicted force time record and the second derivative of the measured force time record at location 13. The forces are in good agreement when a force is being applied, but some large oscillation exists in the predicted record when no force is actually being applied. Careful inspection of the figure reveals that the oscillations have a frequency of 125 Hz, correponding to the frequency of the filter. Figure 5 shows a comparison of the forces at locations 4, 6, and 8. The magnitude of the predicted forces is small relative to the force at point 13 (these records were already scaled using the scaling factor employed at point 13).

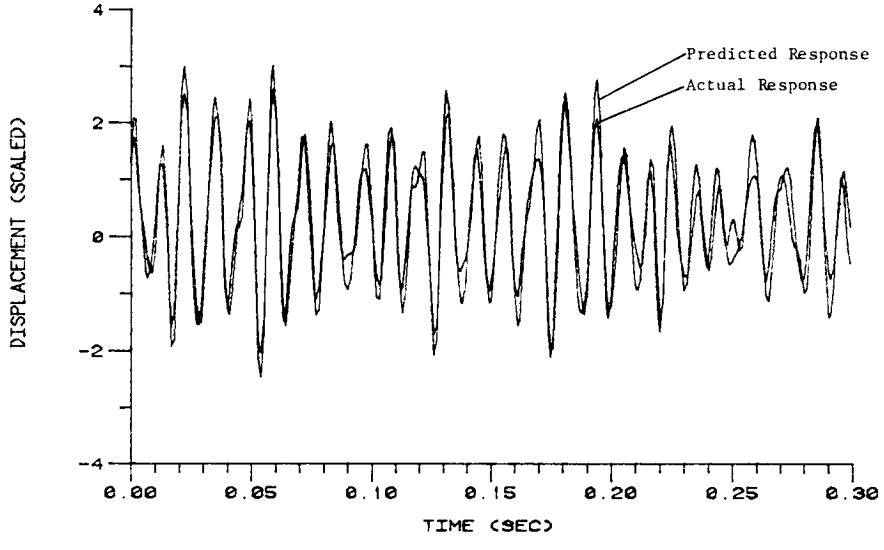

Figure 4 - Comparison of measured vs. predicted forces at point 13

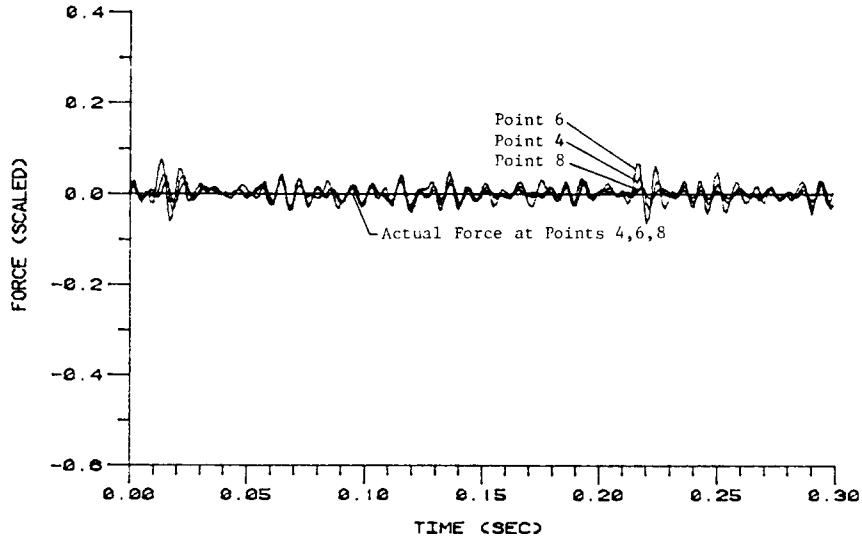

Figure 5 - Comparison of measured vs. predicted forces at points 4,6,& 8.

DAMAGE DETECTION

A useful application for the system identification technique is the detection of changes in the system parameters resulting from induced damage. A large crack in a structure would decrease the local stiffness, thus reducing one or more of its natural frequencies. On the other hand, a corroded section of the structure might reduce the localized mass as well as the stiffness. Therefore, by calculating the system matrices consistently and comparing them to the matrices of the originally perfect system, the occurance of a damage, and possibly its identity, might be detected.

Damage Detection Criterion

Although this approach is theoretically feasible and effective, it is not easy to implement in practice. The difficulty arises in interpreting the changes in the system model and in being able to connect the different changes with the types of damages that could have resulted in their occurrance. In addition, it is possible that some parameters are more meaningful than others in this application. For example, the diagonal elements in the mass matrix are more sensitive to changes in mass at their respective locations than the off diagonal elements.

The stiffness matrix is somewhat more difficult to analyze than the mass matrix. From the point of view of damage detection, it is more appropriate to observe changes in the flexibility matrix than the stiffness matrix. This can be easily verified by considering the static equations describing a multidegree-of-freedom system, namely

$$[K]\,\mathbf{X} = \mathbf{F} \tag{2}$$

Defining the flexibility matrix as $[A] = [K]^{-1}$, Equation (2) becomes

$$\mathbf{X} = [A]\,\mathbf{F} \tag{3}$$

Assuming the system to have three degrees-of-freedom, Equations (2) and (3) may be expanded as follows:

$$\begin{aligned} k_{11}\,x_1 + k_{12}\,x_2 + k_{13}\,x_3 &= f_1 \\ k_{21}\,x_1 + k_{22}\,x_2 + k_{23}\,x_3 &= f_2 \\ k_{31}\,x_1 + k_{32}\,x_2 + k_{33}\,x_3 &= f_3 \end{aligned} \tag{4}$$

and

$$\begin{aligned} x_1 &= a_{11}\,f_1 + a_{12}\,f_2 + a_{13}\,f_3 \\ x_2 &= a_{21}\,f_1 + a_{22}\,f_2 + a_{23}\,f_3 \\ x_3 &= a_{31}\,f_1 + a_{32}\,f_2 + a_{33}\,f_3 \end{aligned} \tag{5}$$

It is clear from Equations (4) that k_{ij} represents the force at point i when $x_j = 1$ and $x_k = 0$ where $k \neq j$. This is rather difficult to visualize in a complex system. On the other hand, it can be seen from Equation (5) that a_{ij} represents the deflection at point i when a unit load is applied at point j. Besides being more physically realizable, any element a_{ij} may be meaningfully treated separately.

The next issue to be addressed is the significance of the diagonal and off-digonal elements in the flexibility matrix. It has been traditionally accepted that only the diagonal terms need to be considered since they strongly reflect the absolute flexibility of their respective locations. This is not necessarily the most effective approach though. To demonstrate that off-diagonal elements are a better indication of the flexibility at a point, consider the system shown in Figure 6a. The beam is of length L and is rigidly attached at both ends. If three equidistant points are monitored on the beam, the resulting flexibility matrix could be found using simple "strength of materials" tables to be

$$[A] = \begin{bmatrix} 2.197 & 2.604 & 1.058 \\ 2.604 & 5.208 & 2.604 \\ 1.058 & 2.604 & 2.197 \end{bmatrix} \frac{10^{-3}\,L^3}{EI}$$

where E is Young's modulus of the material and I is the cross-sectional area moment of inertia of the beam. Now, taking the extreme case, suppose that the beam was cut at some point between locations 1 and 2, resulting in two cantilever beams of unequal lengths (Figure 6b). The new flexibility matrix of the damaged system is

$$[A]^d = \begin{bmatrix} 5.208 & 0.000 & 0.000 \\ 0.000 & 41.667 & 13.020 \\ 0.000 & 13.020 & 5.208 \end{bmatrix} \frac{10^{-3}\,L^3}{EI}$$

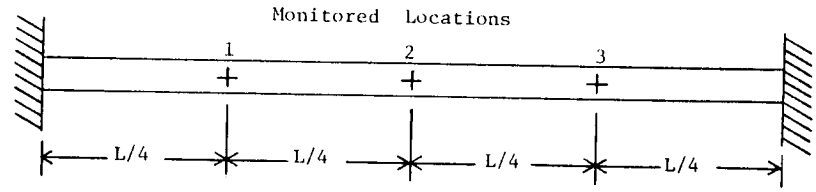

(a)

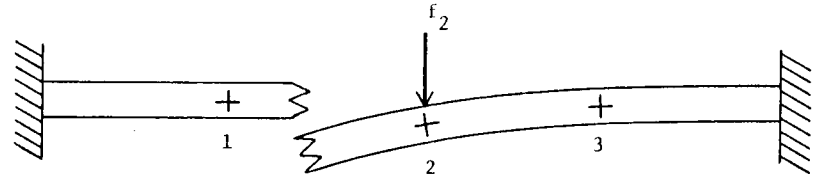

(b)

Figure 6 - a) Configuration of undamaged fixed-fixed beam
b) Configuration of damaged fixed-fixed beam. Separation into two cantilever (fixed-free) beams.

A matrix [R] may now be constructed where each element r_{ij} is defined as

$$r_{ij} = \frac{a^{d}_{ij}}{a_{ij}}$$

namely

$$[R] = \begin{bmatrix} 2.371 & 0.000 & 0.000 \\ 0.000 & 8.000 & 5.000 \\ 0.000 & 5.000 & 2.371 \end{bmatrix}$$

Graphing the diagonal terms as a function of point location (Figure 7a), and noting that the beam ends have a ratio of 1, it would be deduced that the damage occurred at point 2 due to the symmetry. On the other hand, if the off-diagonal elements of the adjacent points are plotted between the two points they represent (Figure 7b), the damage would be correctly identified as being between 1 and 2. It is of vital importance to note that for diagonal terms the steepest peak represents the damage

whereas for off-diagonal terms the steepest valley represents the damage. This is because a load applied at a point next to the damage would cause the point to deflect more than it did before the damage was introduced, whereas the point on the other side of the damage would deflect less than it did before the damage was introduced.

This example may be expanded intuitively to consider the intermediate event where the cut is not severe enough to separate the beam. If the beam is assumed to be composed of two springs, one represnting the portion to the left of the damage, and the other the portion to the right, then the deflection on either side of the damage would be in-directly proportional to its respective spring stiffness. In terms of the flexibility matrix ratio, this would mean that the terms which were zero would begin at 1 when no damage exists, then decrease as the damage size increases, until the limiting value of zero is reached when the cut goes all the way through the beam. Conversely, the off-diagonal terms larger than 1 would begin at unity for no damage and finally reach some finite limiting value for the through cut. Figure 7c depicts this process showing the direction of change in the off-diagonal elements. On the other hand, the ratio of the digonal elements would always result in a symmetric curve regardless of the severity of the damage (Figure 7d).

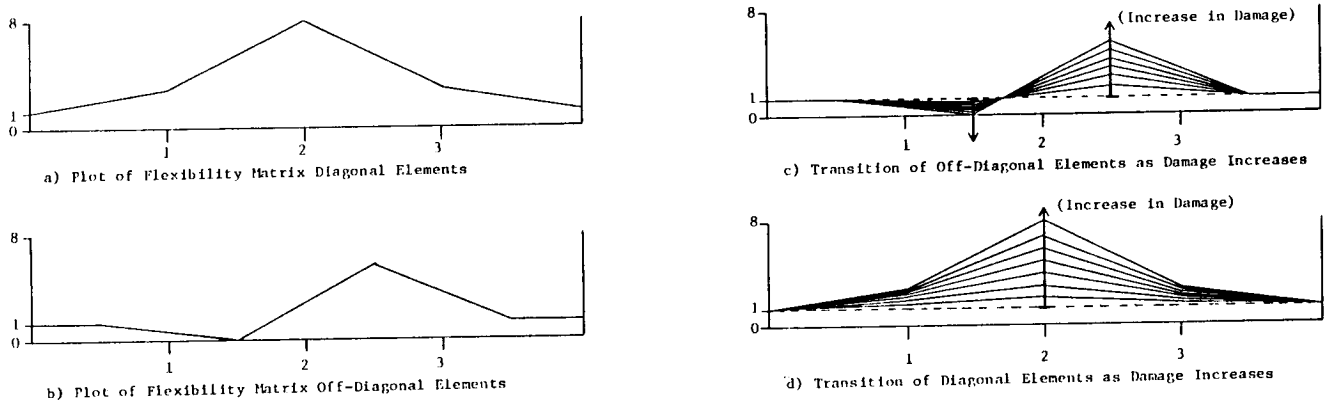

Figure 7

Experimental Implementation of Detection Criterion

An experiment was designed and conducted to verify the accuracy of the proposed damage detection criterion. The experiment was composed of two identical parts, one performed before the damage was induced, and the other afterward. To obtain the response of every labeled point on the structure, each part was actually carried out four times. Since four accelerometers were used, one accelerometer was kept at point

10 while the other three were moved to different locations for each run of the experiment. The four sets of monitored points were (1,2,3,10), (4,5,6,10), (7,8,9,10), and (11,12,13,10). The collected data were processed in the same fashion described earlier.

Since station 10 was common for all the sets, it was used for triggering while cross-Randomdec signatures were obtained for the other points. This resulted in four separate Randomdec signatures. The four signatures, shown in Figure 8, prove the repeatability of the technique.

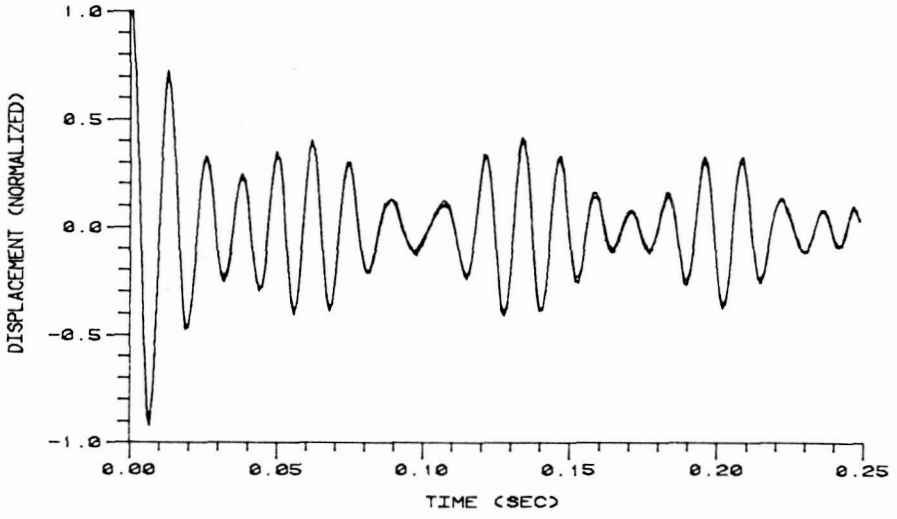

Figure 8 - Comparison of four independently obtained Randomdec signatures at location 10

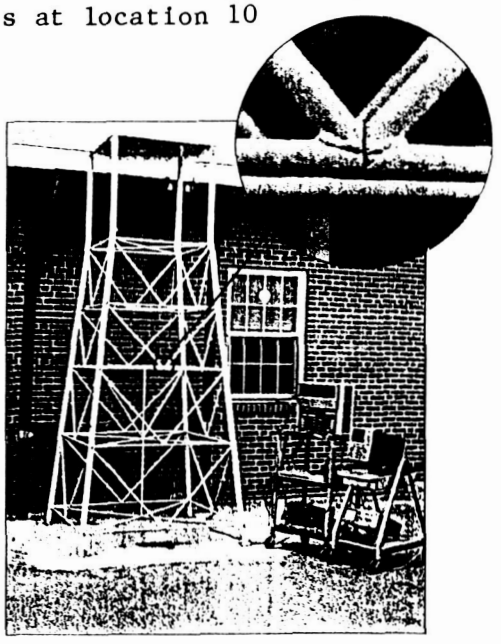

Figure 9 - Location of through cut on offshore platform model

A through cut was made with a hand saw at the cross member between points 5 and 6 (Figure 9). The same process was repeated and twelve cross-Randomdec signatures

calculated. Figure 10 shows the Randomdec signatures at location 10 before and after the damage was induced. The changes in frequency and phase are quite apparent.

The system identification technique was then used in conjunction with the two pairs of Randomdec signatures at point 10 and the two pairs of eleven cross-Randomdec signatures at points 1 to 9, 11, and 12 to obtain the system parameters before and after the damage. This resulted in two pairs of 12x12 [M], [C], and [K] matrices. The two stiffness matrices were inverted yielding two flexibility matrices, and the ratio of the respective elements taken. Table I shows the ratios of the diagonal elements and the off-diagonal elements representing adjacent points. Figure 11 shows the diagonal ratios plotted directly on the structure. It is not clear from the figure where the location of the damage is. The plot of the off-diagonal ratios on the structure is shown in Figure 12. Noting the fact that the lowest ratio indicates the location of the damage, it can be deduced from this figure and from Table I that the damage is residing somewhere between points 5 and 6.

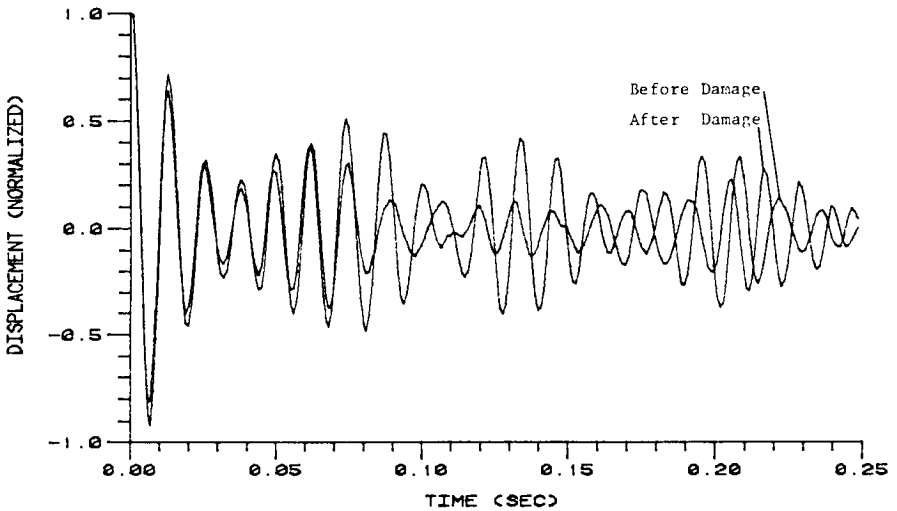

Figure 10 - Change in Randomdec signature at point 10 after damage

Table I - Ratios of flexibility matrix elements before and after damage

DIAGONAL ELEMENTS				OFF-DIAGONAL ELEMENTS					
LEG 1 POINTS		LEG 2 POINTS		LEG 1 MEMBERS		LEG 2 MEMBERS		INTERMEDIATE MEMBERS	
Point Number	Ratio	Point Number	Ratio	Member Number	Ratio	Member Number	Ratio	Member Number	Ratio
1	1.02	2	1.16	1,3	3.08	2,4	3.26	1,2	3.62
3	2.67	4	2.29	3,5	1.76	4,6	1.97	3,4	1.16
5	3.91	6	5.27	5,7	0.87	6,8	0.92	5,6	0.13
7	1.86	8	0.06	7,9	0.53	8,10	0.62	7,8	0.50
9	4.64	10	1.64	9,11	2.56	10,12	2.16	9,10	1.04
11	2.29	12	1.09	-	-	-	-	11,12	3.19

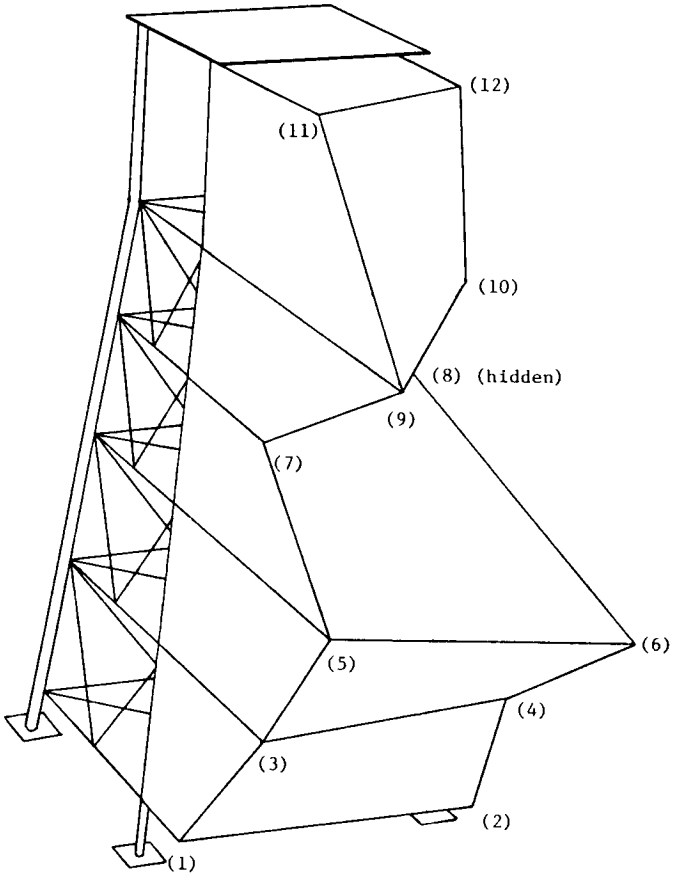

Figure 11 - Plot of flexibility matrix diagonal elements on scale model

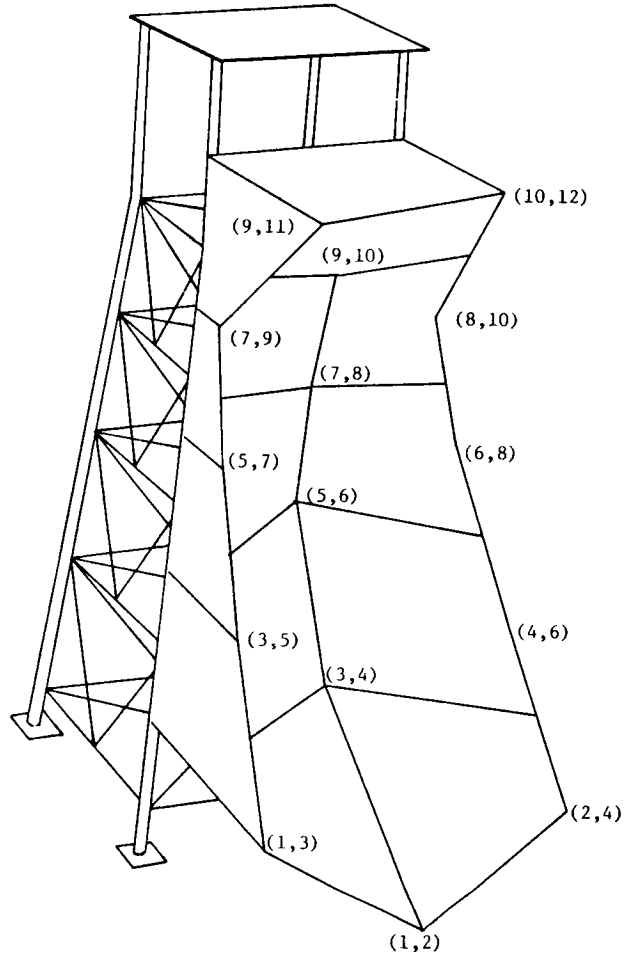

Figure 12 - Plot of flexibility matrix off-diagonal elements on scale model

CONCLUSIONS

An experiment was conducted on a scale model of an offshore platform structure to verify the applicability of the system identification technique introduced in part I of this paper. The technique was employed to obtain a mathematical model of the structure from the random response data. This model was then used to predict the response of the structure and the forcing function initially introduced to excite the structure. These results compared favorably with the measured data.

Finally, an approach to damage detection and location was demonstrated through the inversion and comparison of the stiffness matrix before and after the damage is introduced. The use of a simple example revealed that the off-diagonal elements are more effective in locating the damage than the diagonal elements. The experiment conducted on the scale model of the offshore platform confirmed these findings successfully.

NOMENCLATURE

$[A]$	flexibility matrix
a_{ij}	element ij of flexibility matrix
$[C]$	damping matrix of multiple D.O.F. system
E	Young's modulus
$\mathbf{F}$	input loading vector
f_i	element i of forcing vector
I	area moment of inertia
$[K]$	stiffness matrix of multiple D.O.F. system
k_{ij}	element ij of stiffness matrix
$[M]$	mass matrix of multiple D.O.F system
$[R]$	matrix containing ratio of flexibility matrices
r_{ij}	element ij of matrix [R]
t	time variable
$\mathbf{X}$	position vector of multiple D.O.F. system
x_i	element i of position vector
$\dot{\mathbf{X}}$	velocity vector of multiple D.O.F. system
$\ddot{\mathbf{X}}$	acceleration vector of multiple D.O.F. system

REFERENCES

1. Bedewi, N.E., "The Mathematical Foundation of the Auto and Cross-Random Decrement Techniques and the Development of a System Identification Technique for the Detection of Structural Deterioration", Ph.D. Dissertation, University of Maryland, 1986.

2. Cole, H.A., Jr., "Methods and Apparatus for Measuring the Damping Characteristics of a Structure", United States Patent No.3,620,069, Nov. 16, 1971.

3. Cole, H.A., Jr., "Failure Detection of a Space Shuttle Wing Flutter Model by Random Decrement", NASA TMX-62,041, May 1971.

4. Ibrahim, S.R. "Random Decrement Technique for Modal Identification of Structures", 18th Structures, Structural Dynamics, and Materials Conference, San Diego, CA., March 21-23, 1977.

5. Yang, J.C.S., Aggour, M.S., Dagalakis, N. and Miller, F., "Damping of an Offshore Platform Model by Randomdec Method", Proc. Second ASCE/EMD Specialty Conference on Dynamic Response of Structures, Atlanta, Georgia, January 1981.

6. Yang, J.C.S., Tsai, T., Tsai, W.H., and Chen, R.Z. "Detection and Identification of Structural Damage from Dynamic Response Measurements", 4th Int'l Symp. on Offshore Mechanics and Arctic Engr., Dallas, TX, February, 1985.